UNIVERSITY
OF TRENTO

DIPARTIMENTO DI INGEGNERIA E SCIENZA DELL'INFORMAZIONE

38123 Povo – Trento (Italy), Via Sommarive 14
http://www.disi.unitn.it

ON THE EFFECTS OF THE EXPLOITATION OF SOURCE DIVERSITY IN ASPECT-LIMITED MULTI-VIEW MICROWAVE IMAGING SYSTEMS

D. Franceschini, P. Rocca, M. Benedetti, M. Pastorino, A Massa

January 2011

Technical Report # DISI-11-224

On the Effects of the Exploitation of Source Diversity in Aspect Limited Multi-View Microwave Imaging Systems

Davide Franceschini[1], Paolo Rocca[1], Manuel Benedetti[1], Matteo Pastorino[2], and Andrea Massa[1]

[1]Department of Information and Communication Technology, University of Trento
Via Sommarive 14, I-38050 Trento, Italy
Phone: +39-0461-882057, Fax: +39-0461-882093,
Email: *andrea.massa@ing.unitn.it*, Web-page: www.eledia.ing.unitn.it

[2]Department of Biophysical and Electronic Engineering, University of Genoa
Via Opera Pia 11A, 16145 Genova, Italy
E-mail: *pastorino@dibe.unige.it*

Abstract *– The reconstruction of unknown regions through active microwave imaging techniques requires the retrieval of a large amount of unknown parameters if one aims at fully characterize the electromagnetic properties of the targets under test. Unfortunately, a limited number of independent measurements is available, especially when the scattered field is undersampled because of intrinsic limitations of the imaging setup. In this context, the paper investigates the potentialities of a methodology based on a multi-source illumination as a possible strategy for compensating the reduction of informative field measures and improving the imaging accuracy with respect to single-source experiments.*

Keywords *– Microwave Imaging, Inverse Scattering, Multiresolution, Multi-Source.*

I. INTRODUCTION

Starting from the measurement of the scattered electromagnetic field collected in a non invasive fashion, active microwave imaging techniques are aimed at reconstructing an unknown region by means of suitable inversion procedures. A variety of applications requires the detection and/or the complete characterization of the material properties of the targets under test, such as subsurface monitoring (e.g., [1][2]), non-destructive evaluation and testing [3][4] and biomedical diagnostics [5]-[6].

Unfortunately, many of the arising inverse problems are affected by several theoretical, computational and practical drawbacks. From the point of view of the theoretical drawbacks, ill-posedness, ill-conditioning and non-linearity [7] make the inversion of the scattering data hard to cope with. Therefore, in order to avoid or diminish these problems, a class of approaches considers approximate techniques (as for example in [8]) that also limit the range of the retrievable profiles. Moreover, the solution of the full inverse problem can be in some cases avoided when only the localization of the scatterers has to be provided. Also in this context several methodologies have been proposed (e.g., [9][10]).

However, in many applications of interest a quantitative characterization of the dielectric and conductivity distributions of the sensed region is necessary and the localization or the shaping of the scatterers is not enough. Therefore, suitable non-linear methodologies aimed at exploiting the complex multiple scattering phenomena have to be employed. A widely adopted approach to deal with this class of inverse scattering problems is that based on optimization procedures. The reconstruction of the unknown profiles is recast into a minimization of a suitable cost functional which consists of the superposition of the mismatch between the measured field data and the field scattered by an object with an estimated contrast. In particular, the iterative minimization algorithms have been widely investigated [11]-[13].

In several cases, the inversion strategies have to retrieve a large amount of parameters starting from a limited number of independent measures, fully collectable through multi-illumination/multi-view measurement systems [14][15]. However, the data are usually corrupted by several kind of errors and because of the ill-posedness and the false solution problems, other types of diversity are usually looked for. A widely adopted approach consists in exploiting multi-frequency illuminations (e.g., [16][17]) to excite complementary scattering effects. Multi-view and multi-frequency techniques are the most commonly used strategy to collect scattering data and a limited attention [18] has been devoted to the “source diversity” approach. In this framework, the idea of using different configurations of the probing sources for exciting different scattering phenomena in the domain under test has been preliminary presented in [19].

In this work, the potentialities and the limitations of such a methodology are further investigated. As a matter of fact, a multi-source illumination appears to be profitable to compensate unavoidable measurement errors that usually occur and that possible intrinsic physical limitations of the acquisition setups (such as limited number of views and/or limited angles of view) are not able to mitigate because of the undersampling of the scattered field.

Although an increased amount of information on the investigation domain can be obtained through a multi-source strategy, the scattering data still remain limited for obtaining a detailed reconstruction that satisfies the resolution accuracy constraints. Consequently, the Iterative Multi-Scaling Approach (IMSA) (investigated in [20][21] for the single-source case) has been customized for satisfactorily processing the enlarged multi-source (MS) dataset.

This paper will be structured as follows; in Sect. II the mathematical formulation of the multisource strategy and its integration in the IMSA will be presented; in Sect. III a comparative numerical analysis will be carried out in order to assess the advantages of the proposed approach; in Sect. IV some conclusions will be drawn

II. MATHEMATICAL FORMULATION

Let us consider a two-dimensional scenario for microwave imaging of cylindrical bodies (Fig. 1), where a bounded unknown scatterer is embedded in an homogeneous investigation domain D_I of known characteristics.

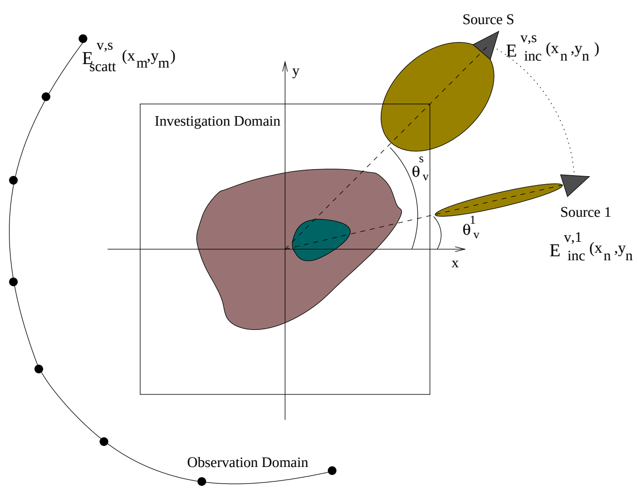

Figure 1. Reference geometry of the tomographic setup.

The contrast of the scatterers with respect to the background can be modeled through the following object function

$$\tau(x,y) = \varepsilon_r(x,y) - 1 - j\frac{\sigma(x,y)}{2\pi f \varepsilon_0} \tag{1}$$

in which $\varepsilon_r(x,y)$ and $\sigma(x,y)$ indicate the relative dielectric permittivity and the electrical conductibility, respectively. Let us suppose that the investigation domain is successively probed from $v = 1,...,V$ different angular positions by means of $s = 1,...,S$ different probing sources characterized by different incident fields ($E_{inc}^{v,s}(x,y)$ being the distribution corresponding to the s-*th* source radiating from the v-*th* angular position). The effects of the interactions between incident fields and the scenario under test are revealed by collecting samples of the scattered electric field through the $m = 1,...,M^{v,s}$ sensors located in the observation domain D_O. The arising scattering phenomena can be described through a pair of integral equations [22], the *Data Equation*,

$$E_{scatt}^{v,s}(x_m^{v,s}, y_m^{v,s}) = k_0^2 \int_{D_I} \Big[\tau(x',y') E_{tot}^{v,s}(x',y') \\ G_{2D}^{ext}\left(x_m^{v,s}, y_m^{v,s} \mid x',y'\right) dx'dy'\Big] \tag{2}$$

defined for $\left(x_m^{v,s}, y_m^{v,s}\right) \in D_O$ and the *State Equation*,

$$E_{inc}^{v,s}(x,y) = E_{tot}^{v,s}(x,y) - k_0^2 \int_{D_I} \left[\tau(x',y') \right. \\ \left. E_{tot}^{v,s}(x',y') G_{2D}^{\text{int}}\left(x,y \mid x',y'\right) dx'dy' \right] \tag{3}$$

defined for $\left(x,y\right) \in D_I$. Eqs. (2) and (3) represent relationships between the problem unknowns [object function $\tau(x,y)$ and internal field $E_{tot}^{v,s}(x,y)$] and the available data [the scattered field $E_{scatt}^{v,s}(x_m^{v,s}, y_m^{v,s})$ and the incident field $E_{inc}^{v,s}(x,y)$]. Moreover, G_{2D}^{ext} and G_{2D}^{int} indicate the external and internal Green's function, respectively. Then, the MS approach allows to define an enlarged set of integral relationships in which the increase of the unknown parameters is limited to those necessary for the representation of the internal field, which has to be reconstructed for each impinging direction and for each of the employed probing sources.

Since the retrieval process is affected by ill-posedness and ill-conditioning, proper countermeasures are needed. Therefore, the inverse problem has to be carefully addressed by properly defining a least-square solution and a suitable regularization strategy. Towards this end, an approach that fully exploits the scattering data from the multi-source acquisition system has been adopted. As a matter of fact, the solution is requested to satisfy the following constraints

$$\phi_{Data}^{(s)}\left\{\tau_{n,1}, E_{tot,n}^{v,s}\right\} = \frac{C_{Data}^{(s)}\left\{\tau_{n,1}, E_{tot,n}^{v,s}\right\}}{c_{Data}^{(s)}} = 0 \tag{4}$$

$$\phi_{Data}^{(s)}\left\{\tau_{n,1}, E_{tot,n}^{v,s}\right\} = \frac{C_{Data}^{(s)}\left\{\tau_{n,1}, E_{tot,n}^{v,s}\right\}}{c_{Data}^{(s)}} = 0 \tag{5}$$

where τ_n and $E_{tot,n}^{v,s}$ indicate the values of the unknowns in the $n = 1,\ldots,N$ subdomains used to discretize the investigation domain.

In Eqs. (4) and (5), $c_{Data}^{(s)}$ and $c_{State}^{(s)}$ are two normalization coefficients defined as follows

$$c_{Data}^{(s)} = \sum_{v=1}^{V} \sum_{m^v=1}^{M^{v,s}} \left| E_{scatt}^{v,s}(x_m^v, y_m^v) \right|^2 \tag{6}$$

$$c_{State}^{(s)} = \sum_{v=1}^{V} \sum_{n=1}^{N} \left| E_{inc}^{v,s}(x_n, y_n) \right|^2 \tag{7}$$

while $C_{Data}^{(s)}\left\{\tau_n, E_{tot,n}^{v,s}\right\}$ and $C_{State}^{(s)}\left\{\tau_n, E_{tot,n}^{v,s}\right\}$ indicate the discretized integral equations

$$C_{Data}^{(s)}\left\{\tau_n, E_{tot,n}^{v,s}\right\} = \sum_{v=1}^{V} \sum_{m^v=1}^{M^{v,s}} \left| E_{scatt}^{v,s}(x_m^v, y_m^v) \right. \\ \left. - \sum_{n=1}^{N} \tau_n E_{tot,n}^{v,s} G_{2D}^{v}(x_m^v, y_m^v \mid x_n, y_n) \right|^2 \tag{8}$$

$$C_{State}^{(s)}\left\{\tau_n, E_{tot,n}^{v,s}\right\} = \sum_{v=1}^{V}\sum_{m^v=1}^{N}\Bigg| E_{inc}^{v,s}(x_n, y_n) - \left[E_{tot,n}^{v,s} - \sum_{p=1}^{N}\tau_n E_{tot,n}^{v,s} G_{2D}^{v}(x_n, y_n \mid x_p, y_p)\right]\Bigg|^2 \tag{9}$$

Hence, starting from the constraints (4)(5) defined for each of the S employed sources the multi-source cost function Φ_{MS} can be defined as

$$\Phi_{MS}\left\{\tau_n, E_{tot,n}^{v,s}\right\} = \Phi_{MS}^{Data}\left\{\tau_n, E_{tot,n}^{v,s}\right\} + \Phi_{MS}^{State}\left\{\tau_n, E_{tot,n}^{v,s}\right\} \tag{10}$$

where

$$\Phi_{MS}^{Data}\left\{\tau_n, E_{tot,n}^{v,s}\right\} = \frac{\sum_{s=1}^{S} C_{Data}^{(s)}\left\{\tau_n, E_{tot,n}^{v,s}\right\}}{\sum_{s=1}^{S} c_{Data}^{(s)}} \tag{11}$$

and

$$\Phi_{MS}^{State}\left\{\tau_n, E_{tot,n}^{v,s}\right\} = \frac{\sum_{s=1}^{S} C_{State}^{(s)}\left\{\tau_n, E_{tot,n}^{v,s}\right\}}{\sum_{s=1}^{S} c_{State}^{(s)}}. \tag{12}$$

According to this approach, the problem unknowns can be reconstructed by minimizing (10) through an available algorithm, whose choice is manifold and independent from the multi-source technique. Thanks to such an approach, one can simultaneously process the enlarged amount of collected scattering-data in order to enhance the reconstruction accuracy by taking into account the different interactions that may occur between scatterer and incident field generated by different electromagnetic sources.

Moreover, the minimization of the MS cost function has been performed profitably integrating the proposed approach into a Multi-Scaling inversion scheme previously proposed for dealing with single-source multi-illumination/multi-view experiments [20][21]. Such an integration is aimed at:

- better exploiting the limited amount of information collected through the multi-source data;
- efficiently dealing with the drawback of the MS approach connected with the unavoidable increase of the unknown parameters of the internal field;
- increasing the ratio between data and unknowns and therefore diminish the false solutions problem.

As a matter of fact, a multi-step $\left(i = 1, \ldots, I_{opt}\right)$ reconstruction process [20] is defined and the following multi-resolution expansion of the unknown profiles is looked for

$$E_{tot}^{v,s,i}(x,y) = \sum_{r_i=1}^{R_i}\sum_{n(r_i)=1}^{N_{(r_i)}} E_{tot}^{v,s,i}(x_{n(r_i)}, y_{n(r_i)})\Omega_{n(r_i)}(x,y) \tag{13}$$

$$\tau_i(x,y) = \sum_{r_i=1}^{R_i}\sum_{n(r_i)=1}^{N_{(r_i)}} \tau_i(x_{n(r_i)}, y_{n(r_i)})\Omega_{n(r_i)}(x,y) \tag{14}$$

in which $\Omega_{n(r_i)}(x, y)$ denotes the n-*th* basis function at the r_i-*th* resolution level of the i-*th* step. The supports of the Regions-of-Interest (*RoIs*) of the investigation domain where the resolution level is increased are defined iteratively and adaptively according to the information that is acquired processing intermediate reconstructions of the object function [20].

III. NUMERICAL ANALYSIS

In this Section, the effectiveness of the multi-source approach is assessed by considering some numerical simulations. As far as the imaging setup is concerned, $M^{v,s} = 27$, $v = 1,...,V$, receivers are located on a semicircular ($\varphi_M = 180^\circ$) observation curve ($r_O = 4\lambda_0$ in radius) located on the left-hand side of an investigation domain $L_{D_I} = 4\lambda_0$-sided. The probing sources are placed on the opposite side and illuminate the scenario from different positions ($V = 4$ directions have been considered) equally spaced in an angular sector ($r_S = 4\lambda_0$ in radius) defined by $\varphi_V = 180^\circ$. Such a setup has been used to probe the scenario characterized by two dielectric cylinders ($\tau = 2.0$) with square cross section ($L_{obj} = 0.53\lambda_0$) located in the investigation area as shown in Fig. 2

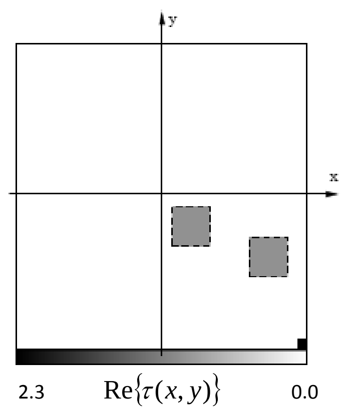

Figure 2. *Multiple scatterers configuration* ($\tau = 2.0$). Reference distribution of the contrast function.

The scattering data have been synthetically-generated by considering the following electromagnetic source models:

Directive Line (DL) source $(s = 1)$ modeled by using an expression similar to the Silver's equation [23]

$$E_{inc}^{v,s=1}(x, y) = -I_o \frac{k_o^2}{8\pi f \varepsilon_0} H_0^{(2)}\left(k_0 \rho_p\right) T(\psi) \tag{15}$$

where $T(\psi) = \sqrt{\sin^3(\psi)}$ if $0 \le \psi \le \pi$ and $T(\psi) = 0$ otherwise, ψ being the polar angle in a coordinate system centered at (x_p, y_p). $H_0^{(2)}$ denotes the second-kind zero-*th* order Hankel function.

Distributed-Line-Currents (DLC) model $(s = 2)$ obtained through a linear array of equally-spaced line-sources, which radiates an electric field given by

$$E_{inc}^{v,s=2}(x, y) = -\frac{k_o^2}{8\pi f \varepsilon_0} \sum_{p=1}^{P} A^s(x_p, y_p) H_0^{(2)}\left(k_0 \rho_p\right) \tag{16}$$

where $A^s(x_p, y_p)$ is an excitation parameter related to the p-*th* element to be set, ρ_p the distance between the point where the field is computed and the p-*th* line source.

As far as the calibration of the excitation parameters is concerned, the coefficients $A^s\left(x_p, y_p\right)$ as well as *P* have been computed through the solution of an inverse-source problem where the known terms were the available samples of $E_{inc}^{v,s}\left(x_m^{v,s}, y_m^{v,s}\right)$ in D_O. More details about the calibration procedure for obtaining the excitation coefficients for the array elements can be found in [24]. In order to obtain a synthesized incident field that is as similar as possible to a real one, the samples of the incident field used in the calibration of the DLC source have been taken from the experimental datasets presented in [25]. Such a tuning allows us to synthesize an incident fields whose distribution inside the investigation domain is shown in Fig. 3 for the impinging direction corresponding to $\theta_{v=1}^{s=2} = 0°$.

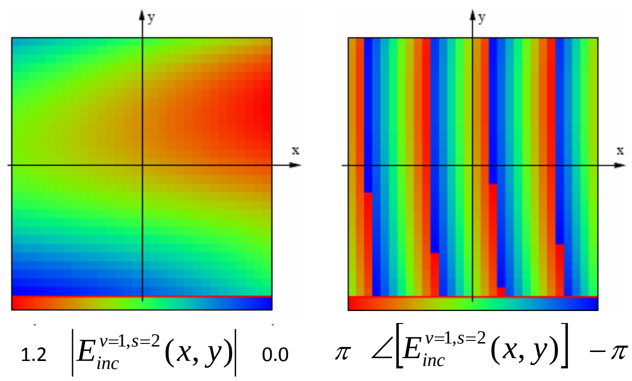

(*a*) (*b*)

Figure 3. Distribution of (*a*) amplitude and (*b*) phase (v=1) of the synthesized *DLC* sources calibrated from experimental measures.

Hertzian Dipole (HD) Source $(s = 3)$ of unitary length positioned at $z = 0$ and radiating in each plane perpendicular to the z axis an incident electric field given by

$$E_{inc}^{v,s=3}(x,y) = I_o \frac{j\eta}{4\pi k_0}\left(\frac{k_0^2}{\rho_p} - \frac{jk_0^2}{\rho_p^2} - \frac{1}{\rho_p^3}\right)e^{-jk_0\rho_p} \tag{17}$$

where $I_0 = 0.1A$ is the intensity of the excitation current.

As far as the reconstruction results are concerned, Fig. 4 shows the retrieved profile through the *IMSA-MS* approach when the data are blurred by means of Gaussian noise with SNR=10 dB. The advantages of processing the enlarged multi-source dataset can be noticed if the previous reconstruction is compared to those obtained by means of the different single source strategies (Fig. 5).

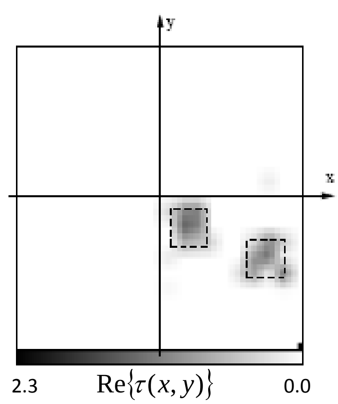

Figure 4. *Multiple scatterers configuration*. Reconstructed dielectric distribution using IMSA-MS (SNR=10 dB - V=4).

As a matter of fact, if on one side the *IMSA-MS* procedure seems moderately affected by the presence of the noise, on the other sides the *SS* strategies obtains less accurate reconstructions (see Tab I and [20] for the definitions of the error figure) also with evident artifacts in the image of the object function (Fig. 5).

The obtained results suggest that the *MS* approach is able to provide an enhanced robustness and stability to the multi-scaling inversion scheme. In order to further verify such aspect, let us also consider a very noisy simulated environment in which SNR=5 dB. For these experiment, the results are reported in a compact fashion through the error figures of Tab. I. Even in these conditions the *IMSA-MS* achieves an acceptable estimation of the contrast ($\chi_{tot}^{MS} = 3.40\%$), while the for the *SS* strategies $\chi_{tot}^{SS} > 6\%$.

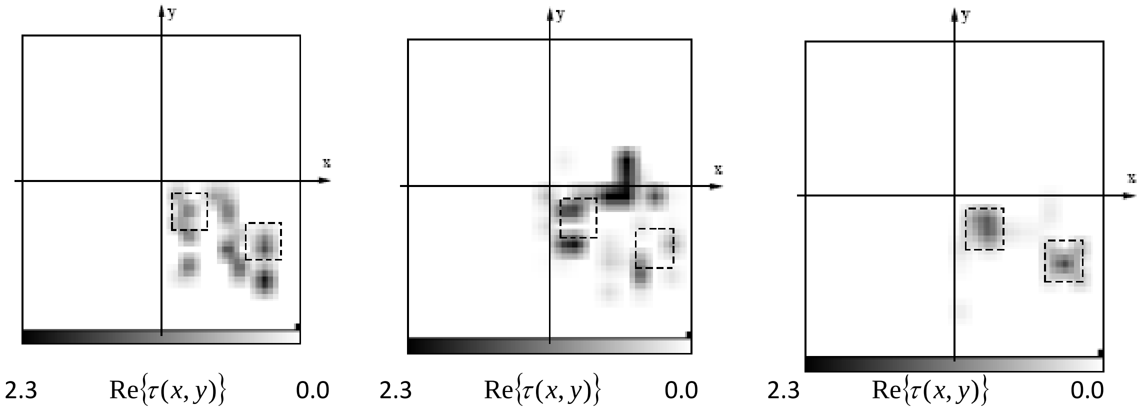

(*a*) (*b*) (*c*)

Figure 5. *Multiple scatterers configuration*. Reconstructed dielectric distribution using (a) IMSA-DL, (b) IMSA-DLC, and (c) IMSA-HD (SNR=10 dB - V=4)

Table I. *Multiple scatterer configuration* (V=4) – Error figures for SNR=10 dB and for SNR=5 dB.

	SNR=10dB			SNR=5dB		
	χ_{tot}	χ_{int}	χ_{ext}	χ_{tot}	χ_{int}	χ_{ext}
MS	1.30	21.50	0.50	3.40	30.20	2.40
SS-DL	7.00	43.60	5.60	9.00	48.50	7.60
SS-DLC	10.00	42.60	8.70	10.80	51.70	9.30
SS-HD	1.40	29.60	0.40	6.00	28.70	5.10

IV. CONCLUSIONS

A new multi-source technique for the acquisition of the information has been numerically tested in order to investigate whether different scattering interactions in the targets under test excited using probing sources with different characteristics can be exploited to improve the imaging accuracy of the multi-scaling approach. Moreover, the integration of the proposed MS approach in the *IMSA* has allowed to obtain a satisfactory trade-off between the achievable spatial resolution accuracy and the limited amount of information collectable during the data acquisition. Thanks to this multi-resolution procedure, the increase of the amount of unknown parameters has been limited, favorably affecting the computational burden and the false solution problem. Furthermore, the proposed multi-source multi-scaling methodology has shown a satisfactory accuracy in quantitatively reconstructing the considered test case and the numerical simulations have pointed out how the multi-source illumination can compensate the reduction of data when multi-view systems present some limitations, providing an enhanced robustness when the data are corrupted by a gaussian noise.

REFERENCES

[1] A. Abubakar and P. M. van den Berg, "Three-dimensional nonlinear inversion in crosswell electrode logging," *Radio Sci*., vol. 4, pp. 989-1004, 1998.

[2] Y. Yu, T. Yu, and L. Carin, "Three-dimensional inverse scattering of a dielectric target embedded in a lossy half-space," *IEEE Trans. Geosci. Remote Sensing*, vol. 42, pp. 957-973, 2004.

[3] J. Ch. Bolomey, *Frontiers in Industrial Process Tomography*. Engineering Foundation, 1995.

[4] M. Benedetti, M. Donelli, G. Franceschini, M. Pastorino, and A. Massa, "Effective exploitation of the a priori information through a microwave imaging procedure based on the SMW for NDE/NDT applications," *IEEE Trans. Geosci. Remote Sensing*, vol. 43, pp. 2584-2592, Nov. 2005.

[5] P. M. Meaney, M. W. Fanning, Li Dun, S. P. Poplack, and K. D. Paulsen, "A clinical prototype for active microwave imaging of the breast," *IEEE Trans. Microwave Theory Tech.*, vol. 48, pp. 1841-1853, 2000.

[6] J. M. Sill and E. C. Fear, "Tissue sensing adaptive radar for breast cancer detection - Experimental investigation of simple tumors models," *IEEE Trans. Microwave Theory Tech.*, vol. 53, pp. 3312-3319, 2005.

[7] A. M. Denisov, *Elements of theory of inverse problems*. Utrecht, The Netherlands: VSP, 1999.

[8] J. B. Keller, "Accuracy and validity of Born and Rytov approximations," *J. Opt. Soc. Am.*, vol. 6, pp. 1003-1004, 1969.

[9] H. Tortel, G. Micolau, and M. Saillard, "Decomposition of the time reversal operator for electromagnetic scattering," *J. Electromagn. Waves Appl.*, vol. 13, pp. 687-719, Mar. 1999.

[10] O. M. Bucci, A. Capozzoli, and G. D'Elia, "A novel approach to scatterer localization problem," *IEEE Trans. Antennas Propagat.*, vol. 51, pp. 2079-2090, Aug. 2003.

[11] R.E. Kleinman and P. M. van den Berg, "A modified gradient method for two-dimensional problems in tomography," *J. Comput. Appl. Math.*, vol. 42, pp. 17-35, 1992.

[12] P. M. van den Berg and R. E. Kleinman, "A contrast source inversion method," Inverse Problems, vol. 13, pp. 1607-1620, 1997.

[13] M. Donelli and A. Massa, "A computational approach based on a particle swarm optimizer for microwave imaging of two-dimensional dielectric scatterers," *IEEE Trans. Microwave Theory Tech.*, vol. 53, no. 5, pp. 1761-1776, 2004.

[14] O. M. Bucci and T. Isernia, "Electromagnetic inverse scattering: retrievable information and measurements strategies," *Radio Sci.*, pp. 2123-2138, 1997.

[15] O. M. Bucci, L. Crocco, T. Isernia, and V. Pascazio, "Subsurface Inverse Scattering Problems: Quantifying Qualifying and Achieving the Available Information", *IEEE Trans. Geosci. Remote Sens.*, vol. 39, pp. 2527-2538, 2001.

[16] K. Belkebir, R. Kleinman, and C. Pichot, "Microwave imaging - Location and shape reconstruction from multifrequency scattering data," *IEEE Trans. Microwave Theory Tech.*, vol. 45, pp. 469-475, 1997.

[17] O. M. Bucci, L. Crocco, T. Isernia, and V. Pascazio, "Inverse Scattering Problems with Multifrequency Data: Reconstruction Capabilities and Solution Strategies," *IEEE Trans. Geosci. Remote Sensing*, vol. 38, pp. 1749-1756, 2000.

[18] S. Caorsi, A. Massa, and M. Pastorino, "Numerical assessment concerning a focused microwave diagnostic method for medical applications," *IEEE Trans. Antennas Propagat.*, vol. 48, pp. 1815-1830, 2000.

[19] D. Franceschini and A. Massa, "On the Enhancement of the Reconstruction Accuracy obtained with a Multi-Source/Multi-Illumination Inverse Scattering Technique," *IEEE Antennas and Wireless Propagat. Lett.*, vol. 4, pp. 194-197, 2005.

[20] S. Caorsi, M. Donelli, D. Franceschini, and A. Massa, "A new methodology based on an iterative multiscaling for microwave imaging," *IEEE Trans. Microwave Theory Tech.*, vol. 51, pp. 1162-1173, 2003.

[21] S. Caorsi, M. Donelli, and A. Massa, "Detection, location, and imaging of multiple scatterers by means of the iterative multiscaling method," *IEEE Trans. Microwave Theory Tech.*, vol. 52, pp. 1217-1228, 2004.

[22] D. Colton and R. Krees, *Inverse Acoustic and Electromagnetic Scattering Theory*, Berlin, Germany: Springer-Verlag, 1992.

[23] C. A. Balanis, *Antenna Theory: Analysis and Design*. New York: Wiley, 1997

[24] R. Azaro, M. Donelli, D. Franceschini, and A. Massa, "An Experimental Study on the Multiscaling Iterative Reconstruction of Inhomogeneous Targets," *Microwave Optical Tech. Lett.*, vol. 47, pp. 588-594, 2005.

[25] K. Belkebir and M. Saillard, Special section: "Testing Inversion Algorithms against Experimental Data," *Inverse Problems*, vol. 17, pp. 1565-1702, 2001.